Combustion and Flame 198 (2018) 169–175

Contents lists available at ScienceDirect

Combustion and Flame

journal homepage: www.elsevier.com/locate/combustflame

Effect of paraffin wax on combustion properties and surface protection of Al/CuO-based nanoenergetic composite pellets

Kyung Joo Kim[a], Myung Hoon Cho[a], Ji Hoon Kim[b], Soo Hyung Kim[a,b,c,*]

[a] Department of Nano Fusion Technology, College of Nanoscience and Nanotechnology, Pusan National University, 30 Jangjeon-dong, Geumjung-gu, Busan 609-735, Republic of Korea
[b] Research Center for Energy Convergence Technology, Pusan National University, 30 Jangjeon-dong, Geumjung-gu, Busan 609-735, Republic of Korea
[c] Department of Nanoenergy Engineering, College of Nanoscience and Nanotechnology, Pusan National University, 30 Jangjeon-dong, Geumjung-gu, Busan 609-735, Republic of Korea

ARTICLE INFO

Article history:
Received 3 April 2018
Revised 10 June 2018
Accepted 10 September 2018

Keywords:
Energetic materials
Thermite
Polymer binder
Aluminothermic reaction
Combustion properties
Surface protection

ABSTRACT

We systematically investigated the effect of a polymer binder on various combustion properties and surface protection of nanoenergetic composite pellets containing Al and CuO nanoparticles (NPs) as the fuel and oxidizer, respectively. Al/CuO NP-based composite pellets were then fabricated by a pelletization process and the effect of paraffin wax (PW) binder concentration was investigated. The burn rate decreased with increasing PW content as the binder thermochemically interfered with the aluminothermic reaction between Al and CuO. However, the presence of a critical amount of PW (< 20 vol% in the Al/CuO matrix) maintained, or even enhanced, the various combustion properties of Al/CuO composite pellets, including the total heat energy, maximum pressure, and pressurization rate, when they were ignited. Simultaneously, the presence of PW was also found to effectively protect Al/CuO pellets from severe oxidation under relatively high humidity conditions. This suggests that PW played key roles as an effective binder, versatile lubricant, and oxidation protection agent. In addition, it could also be used for controlling the combustion properties of nanoenergetic material-based pellets for various thermal engineering applications.

1. Introduction

Energetic materials (EMs) consist of a fuel and an oxidizer and show an intense exothermic reaction due to a violent oxidation process. Aluminum is generally used as the fuel because it is relatively stable, abundant, and inexpensive. Various materials have been used as the oxidizer, such as NiO, TiO_2, WO_3, MoO_3, Fe_2O_3, and $KMnO_4$, which can vary the combustion properties of EMs by tailoring the degree of mixing, chemical composition, and physical structure [1–4]. The strong self-sustained exothermic reaction of EMs is accompanied by a relatively high temperature when they are ignited by external energy input. The typical aluminothermic reaction takes place as follows [5–7]:

$$2Al + 3MO \rightarrow Al_2O_3 + 3M + \Delta H \quad (1)$$

where MO is a metal oxide, M is a metal, and ΔH is the generated heat energy. Conventional EMs have some limitations for practical thermal engineering applications, including their relatively low reaction rate and mass transfer between the fuel and oxidizer. Numerous studies have been performed that aimed to improve these properties using nanostructured materials, which increase the interfacial contact area between reacting materials [8–14].

Enhanced stability and insensitivity of EMs can be achieved by either passivating the surface of fuel particles or coating EMs with organic materials; however, this deteriorates their combustion properties to some extent [15–24]. Generally, Al particles have an oxidation layer on their surfaces after exposure to oxidizing atmospheres. The formation of this oxidation layer on Al particles plays a key role in their passivation [25–33]. In the case of Al NPs, a greater relative volume of oxidation product is formed due to the higher specific surface area compared to larger particles; hence, the relative volume of the reacting core is reduced, which eventually results in significant degradation of the combustion properties [34,35]. Jelliss et al. [36] reported a synthesis method for hydrogen-evolving polymer-capped Al NPs using $LiAlH_4$ (lithium aluminum hydride), which was designed to protect Al from oxidation. The polymeric binders coating the surface of Al NPs protected them from rapid oxidation; however, the energy re-

* Corresponding author at: Department of Nano Fusion Technology, College of Nanoscience and Nanotechnology, Pusan National University, 30 Jangjeon-dong, Geumjung-gu, Busan 609-735, Republic of Korea.
E-mail address: sookim@pusan.ac.kr (S.H. Kim).

https://doi.org/10.1016/j.combustflame.2018.09.010
0010-2180/

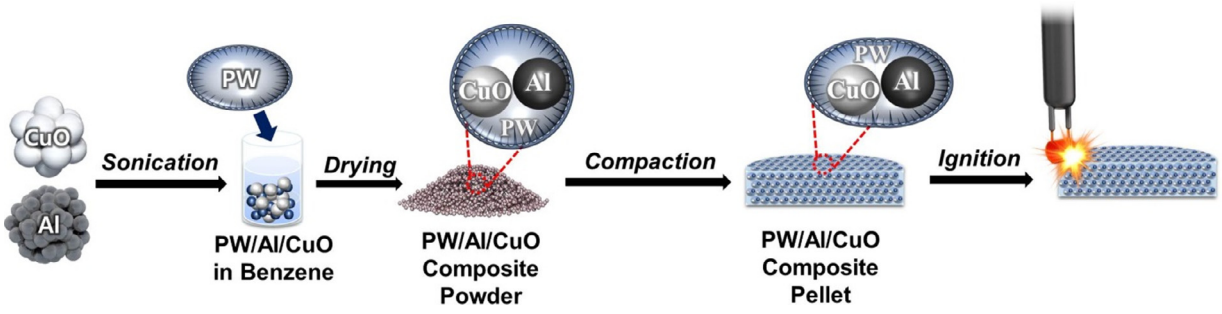

Fig. 1. Schematic diagram of the fabrication and ignition of PW/Al/CuO composite pellets.

lease rate was also significantly reduced. Gangopadhyay et al. [37] successfully synthesized nanoenergetic materials (nEMs) composed of self-assembled structures of poly (4-vinylpyridine)-coated Al NPs and CuO. They increased the energy release rate of nEMs using unique nanostructures of fuel, oxidizer, and polymeric binder; this was effective for powders, but not for preparation of pellets as the reactivity of the pellets was significantly reduced due to the lower specific surface area resulting from the compressive forces applied during pelletization. Since EM powders are not easy to handle, EM-based pellets are preferred for the various thermal engineering applications. Unlike EM powders, the fabrication and combustion properties of EM-based pellets are strongly affected by various parameters, including the theoretical density, particle size, and polymer additives.

In this study, we systematically examined the effects of a polymer additive (paraffin wax; PW) as a binder, desensitizing agent, and oxygen/water protectant for EMs on the combustion properties of nEM-based pellets. Specifically, we used Al NPs and CuO NPs as the fuel and oxidizer, respectively. Various combustion properties of polymer-added nEMs pellets were systematically investigated, including heat energy, pressure trace, pressurization rate, burn rate, and total burning time.

2. Materials and methods

Figure 1 shows schematic diagrams of the fabrication and ignition processes of the PW/Al/CuO composite powders and pellets. Briefly, Al and CuO NPs were mixed with a ratio of 30:70 wt% in an ethanol solution, which was then sonicated (ultrasonic power = 170 W, ultrasonic frequency = 40 kHz) for 30 min. Al/CuO NP-based powders were obtained by drying the ethanol solution in a convection oven at 80 °C for 30 min. PW was dissolved in ~50 mL benzene solution with various mixing ratios (0, 10, 20, 30, 40, and 50 vol%), and then dispersed ultrasonically after addition of Al and CuO NPs.

To measure the heat energy generated by the aluminothermic reaction in the as-prepared PW/Al/CuO composite powders, differential scanning calorimeter (DSC; Setaram, Model No. LABSYS evo) analysis was performed under a nitrogen atmosphere with a heating rate of 10 °C min^{-1} between 30 and 1000 °C. To measure the combustion properties of PW/Al/CuO composite pellets, 100 mg of the composite powder was first formed into a disk-shaped pellet with a diameter of 7 mm and height of 0.7 mm at a pressure of ~300 MPa. The surface of the composite pellets was then observed using field-emission scanning electron microscopy (FE-SEM; Hitachi, Model No. S4700) at ~15 kV. To observe the combustion reactivity of PW/Al/CuO composite pellets ignited in ambient air, a high-speed camera (Photron, FASTCAM SA3 120 K) was used with a frame rate of 30 kHz. This camera had a maximum frame rate of 1,200,000 fps, minimum frame rate of 60 fps, CMOS image sensor size of 17.4 mm × 17.4 mm, and pixel size of 17 µm × 17 µm.

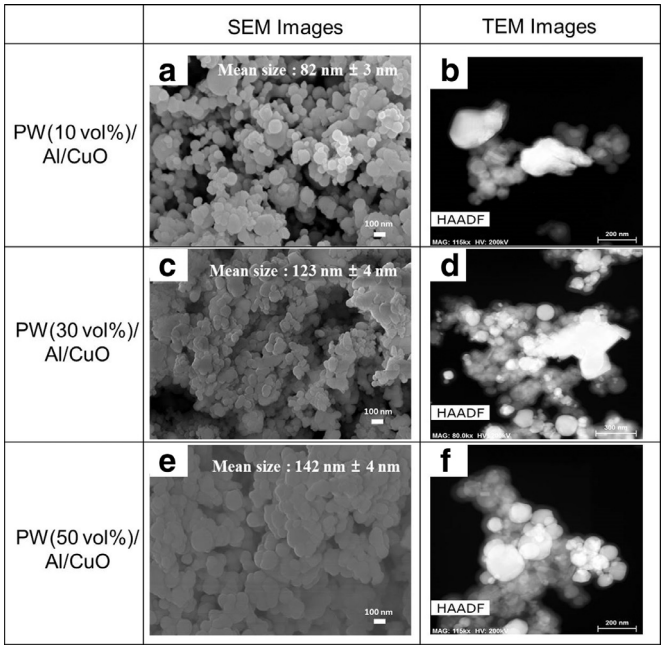

Fig. 2. SEM and TEM images of (a) & (b) PW(10 vol%)/Al/CuO, (c) & (d) PW(30 vol%)/Al/CuO, (e) and (f) PW(50 vol%)/Al/CuO composite powders.

In order to investigate the influence of the PW binder on the combustion properties of Al/CuO-based nEMs, the pressure curves and the pressurization rate were examined using a pressure cell tester (PCT). We placed ~26 mg of a PW/Al/CuO composite pellet in the PCT system, which was then ignited and exploded using a tungsten hot-wire. The pressure sensor system consisted of a pressure sensor (PCB piezotronics, Model No. 113A03) with a maximum detection pressure of ~15 kpsi, a signal amplifier (PCB piezotronics, Model No. 422E11) and an oscilloscope (Tektronix, TDS 2012B). The water permeability of the PW/Al/CuO composite pellets was estimated using a sessile drop method, where 10 µL of deionized water was dropped on the surface of the pellet and the contact angle of the droplet was measured using a CCD camera.

3. Results and discussion

FE-SEM analysis was performed to examine the size, shape, and homogeneity of PW/Al/CuO composites, as shown in Fig. 2. Figure 2a shows that highly aggregated Al/CuO composite NPs with an average diameter of ~82 ± 3 nm were formed. Al and CuO NPs were closely bound to each other in the PW matrix as shown in Fig. 2b. The elemental mappings were provided in **Fig. S1** in the supporting information. The primary size of the Al/CuO composite powder increased with increasing the amount of PW in the

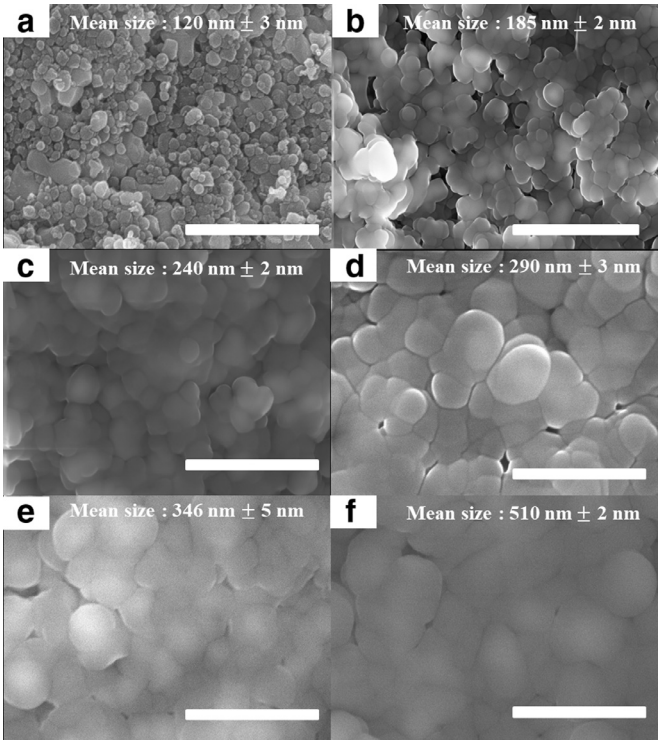

Fig. 3. FE-SEM images of cross-sectional views of (a) PW(0 vol%)/Al/CuO, (b) PW(10 vol%)/Al/CuO, (c) PW(20 vol%)/Al/CuO, (d) PW(30 vol%)/Al/CuO, (e) PW(40 vol%)/Al/CuO, (f) PW(50 vol%)/Al/CuO composite pellets. (The scale bars indicate 1 μm.)

Al/CuO matrix, as shown in Fig. 2c and e, where the average diameters of the PW(10 vol%)/Al/CuO, PW(30 vol%)/Al/CuO, and PW(50 vol%)/Al/CuO were ~82 ± 3 nm, ~123 ± 4 nm, and ~142 ± 4 nm, respectively. Based on closer observation for TEM images as shown in Fig. 2b, d, and f, the thickness of PW coating layer was also increased to 19 nm, 22 nm, 32 nm as the PW content was increased with 10, 30, and 50 vol%, respectively. This suggests that the Al/CuO composites were uniformly coated by PW binder so that the primary sizes of Al/CuO reacting particles were increased with increasing the amount of PW binder.

Figure 3 shows FE-SEM images of cross-sections of PW/Al/CuO composite pellets with various amounts of added PW. Figure 3a shows the cross-sectional view of an Al/CuO composite pellet without added binder (PW(0 vol%)/Al/CuO pellet). As the amount of PW added into Al/CuO matrix increased, the primary size of the Al/CuO composite significantly increased and simultaneously, the boundaries between primary particles disappeared, as shown in Fig. 3b–f. The PW binder used here had a relatively low molecular weight and good flow properties and was present on the surface of Al/CuO NPs; hence, the primary size of the composite pellets was much larger than that of the initial powders due to the compressive forces during the pelletization process. In addition, the number of pores between the primary particles decreased with increasing PW content. This suggested that the binder-coated Al/CuO composites in the pellets were plastically deformed and strongly bonded, resulting in increased the relative density of the composite pellet with increasing PW content.

We examined the influence of PW content on the relative density of the prepared composite pellets. Figure 4 shows the relative density (D_r) as a function of PW content in Al/CuO composite pellets. The theoretical density (D_{th}) was determined by the mixing rule, where the theoretical density of a composite with three components can be defined as follows:

$$D_{th} = (W_1 + W_2 + W_3)/(W_1/D_1 + W_2/D_2 + W_3/D_3) \quad (2)$$

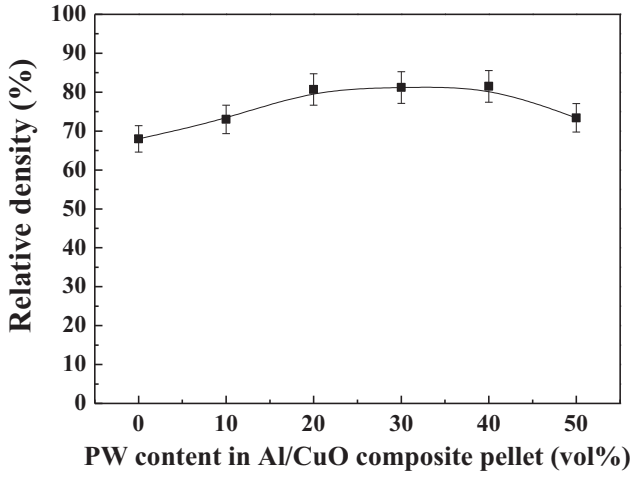

Fig. 4. Evolution of the relative density of PW/Al/CuO composite pellets as a function of PW content.

In this case, W_1, W_2, and W_3 were 0, 0.3, and 0.7 wt%, corresponding to the PW, Al, and CuO NPs, respectively, while D_1, D_2, and D_3 were 0.9 g cm^{-3}, 2.7 g cm^{-3}, and 6.3 g cm^{-3}, corresponding to the PW, Al NPs, and CuO NPs, respectively. Based on Eq. (1), the resulting theoretical density of the Al/CuO composite without PW was ~4.5 g cm^{-3}. The theoretical density of PW/Al/CuO composite pellets with different PW contents of 0, 10, 20, 30, 40, and 50 vol.% were approximately 4.50, 4.14, 3.78, 3.42, 3.06, and 2.70 g cm^{-3}, respectively. The measured density of the composite pellets fabricated here was determined from the ratio of measured weight to volume, and the relatively density was finally determined by dividing the measured density by the theoretical density. The D_r of the Al/CuO pellets without PW was ~68%, which was relatively low as the compressive force applied during pelletization process was reduced by the presence of large frictional forces among the Al/CuO NPs. However, the frictional force decreased with increasing binder content in the Al/CuO matrix, resulting in significantly increasing D_r values, which peaked at ~80% for a PW binder content of 40 vol.%. The addition of PW to the Al/CuO matrix played key roles as both a lubricator and binder during pelletization. Hence, a higher relative density of the PW(10-40 vol%)/Al/CuO composite pellet was obtained due to strong bonding between the Al/CuO particles when the PW content increased. However, when the amount of PW exceeded 50 vol%, D_r suddenly decreased to 73%. This was presumably because the excessive amount of PW separated the distances between Al/CuO composite clusters too much by occupying a larger specific volume in the pellets.

The ignition and combustion properties of PW/Al/CuO composite pellets were observed in-real time using a high-speed camera, and then the burn rate and total burning time were determined experimentally via video and still image analyses. The flame propagation images of various PW/Al/CuO composite pellets ignited using a tungsten wire are summarized in Fig. 5. The burn rate was determined from the diameter of the composite pellet divided by the total time required for propagating the flame from one end to the other. As shown in Fig. 5a, ignition and combustion successfully occurred for all samples. Ignition was initiated at one end of the pellets using a hot tungsten wire, and the generated flame rapidly propagated throughout the pellets; macroscopic combustion and explosion were accompanied by the aluminothermic reaction. Figure 5b shows the burn rate and total burning time of PW/Al/CuO composite pellets analyzed using still images taken using the high speed camera. The burn rates of PW/Al/CuO

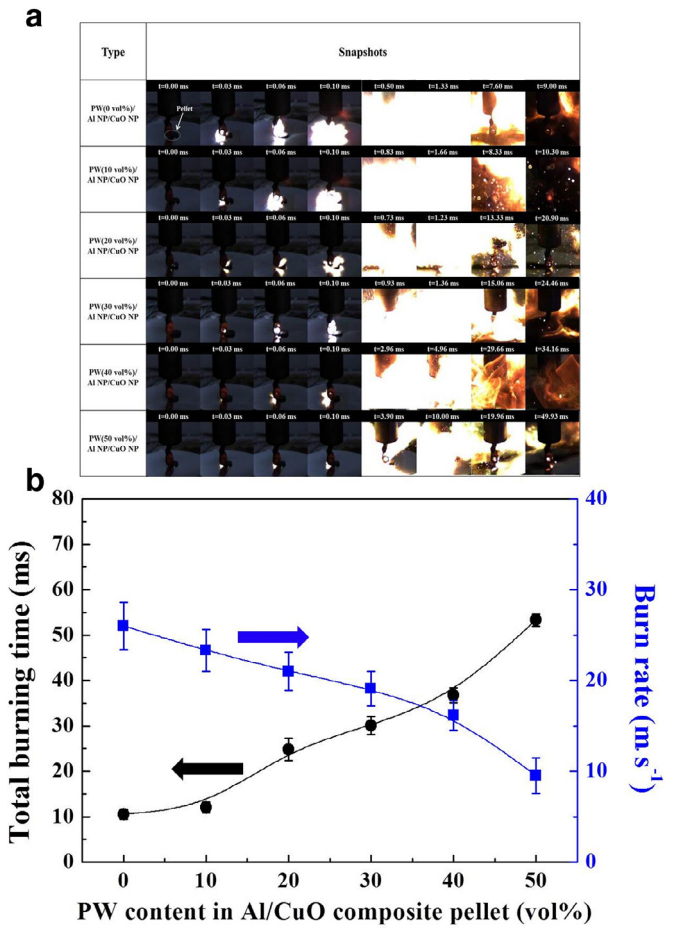

Fig. 5. (a) Snapshots of tungsten hot-wire-assisted ignition of PW/Al/CuO composite pellets with different PW contents. The pixels of the still images in the third column were commonly overloaded due to the flash generated by pellet combustion. (b) Burn rate and total burning time of PW/Al/CuO composite pellets as a function of PW content.

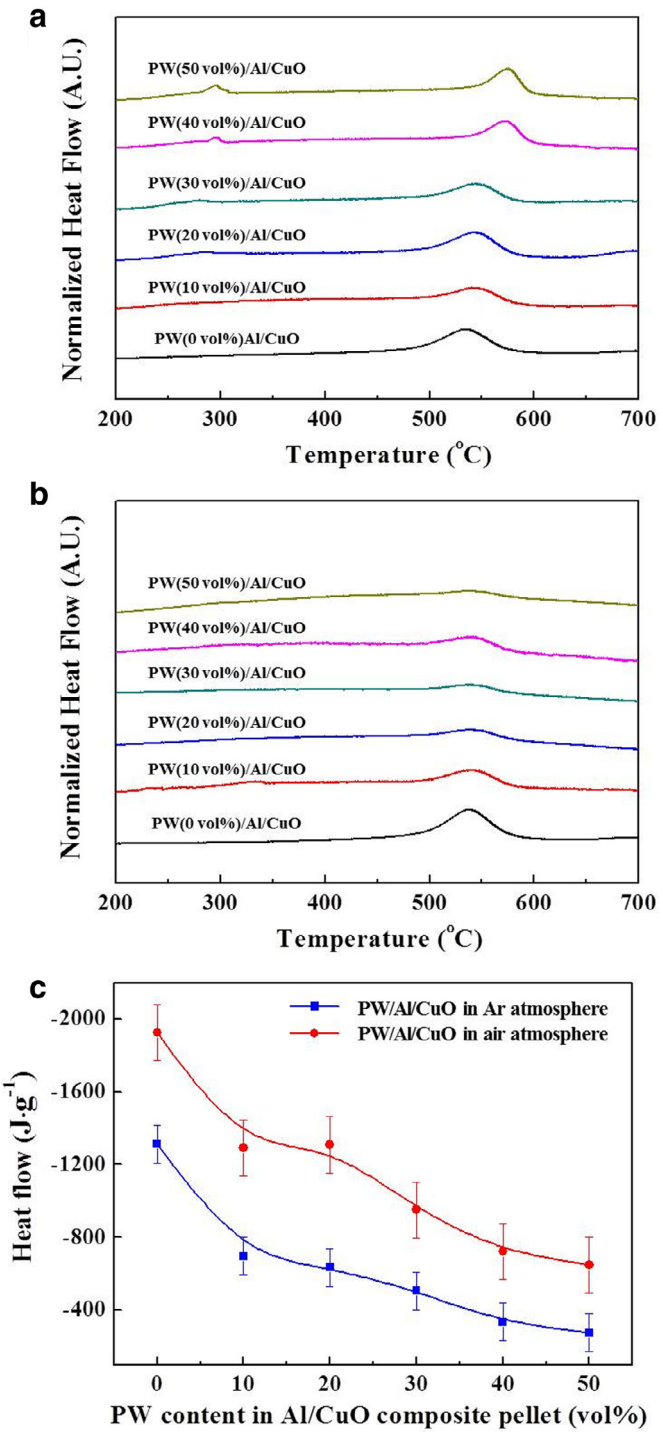

Fig. 6. (a) DSC heat flow curves of the PW/Al/CuO/composites measured in (a) an air and (b) Ar atmosphere, and (c) evolution of total exothermic heat energy as a function of added PW content in the Al/CuO composite pellets.

composite pellets with PW contents of 0, 10, 20, 30, 40, and 50 vol% were approximately 26.00, 23.30, 21.00, 19.09, 16.15, and 9.54 m s^{-1}, respectively. As the PW content increased, the burn rate decreased as the distance between Al and CuO NPs increased; hence, the heat and mass transfer rates were retarded in the pellets. In addition, the thermal energy generated by the aluminothermic reaction was used by binder combustion, which interfered with thermal energy transfer. Higher PW contents added to the Al/CuO matrix resulted in slower burn rates, resulting in longer total burning times (Fig. 5b). In addition, a series of burn tube tests were also performed to corroborate the combustion properties of PW/Al/CuO composite powders, and then we observed that the evolution of burn rate and total burning time of the composite powders were very similar with the results of the composite pellet ignition tests as shown in **Fig. S2** in the supporting information. This suggests that the presence of PW contents can significantly perturb the combustion characteristics of Al/CuO composites.

To examine the effect of the amount of PW on the exothermic reaction of Al/CuO composites, DSC analyses were performed for different PW/Al/CuO composites in an air atmosphere (Fig. 6a). It can be seen that there were two predominant exothermic reactions; the first occurred at 250–350°C due to PW oxidation (i.e., $C_{25}H_{52} + 38O_2 \rightarrow 25CO_2 + 26H_2O + \text{Heat}$) and the second exothermic reaction generally occurred at 450–600°C due to the aluminothermic reaction between Al and CuO NPs. To additionally examine the heat energy release of the composites in the oxygen lean environment, the DSC analyses were separately performed in an Ar atmosphere (Fig. 6b). Unlike the DSC results performed in the air, the first exothermic reaction occurred at 250–350°C was disappeared. This suggests that the oxidation reaction of PW was not occurred because there was no oxygen in the Ar atmosphere. The PW/Al/CuO composites were observed to commonly exhibit the exothermic reactions occurred at 450-600°C in the Ar atmosphere. PW is typically known to have a melting point of ~70 °C, a boiling point of ~370 °C, and has a heat of fusion of

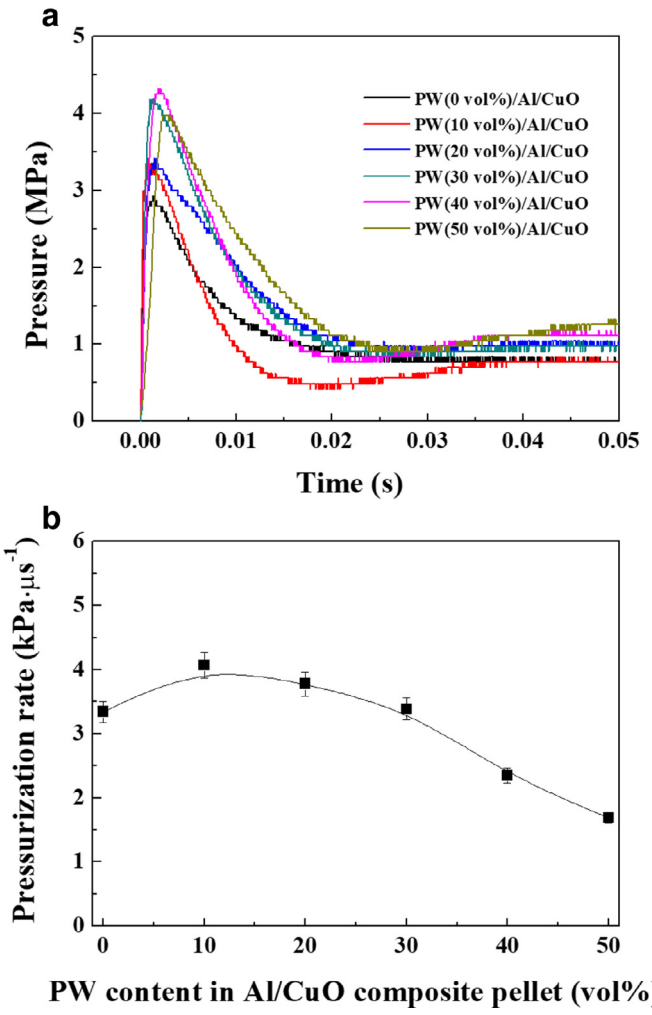

Fig. 7. (a) Pressure traces and (b) pressurization rates of PW/Al/CuO composite pellets as a function of PW content.

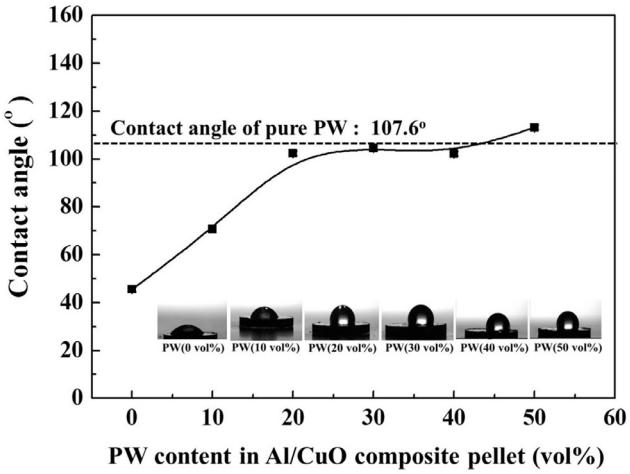

Fig. 8. Evolution of the contact angle of PW/Al/CuO composite pellets as a function of PW content in the Al/CuO composite pellets. (Inset are photographs of contact angle measurements for the different samples.)

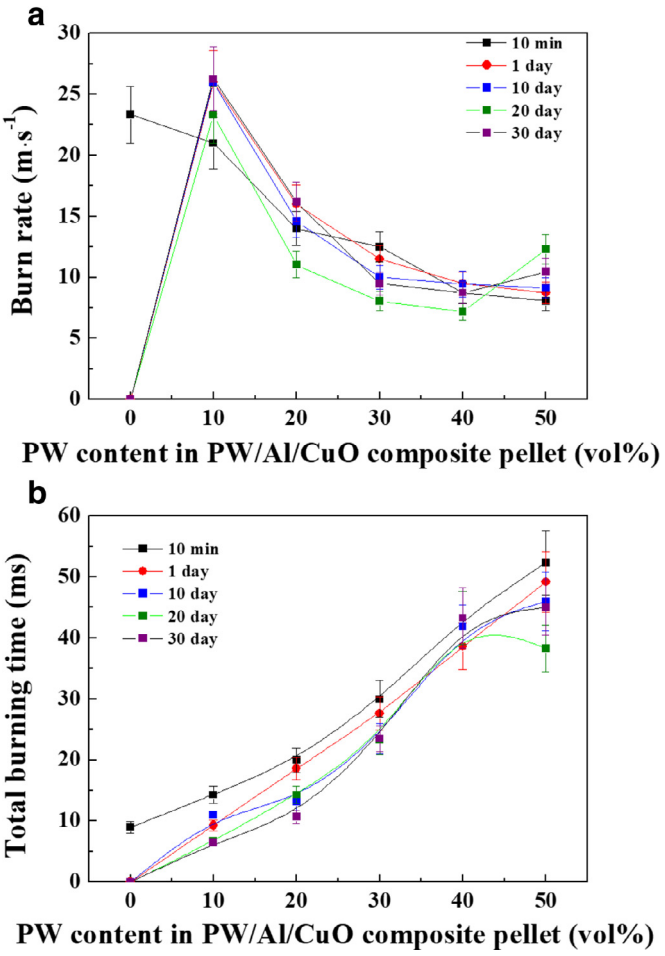

Fig. 9. Evolution of (a) burn rates and (b) total burning time of various PW/Al/CuO pellets exposed to a fixed RH of 50% for various durations.

~200–220 J•g^{-1}. Therefore, as the temperature increased, the PW was turned into liquid state at ~70 °C, and then it was turned into gas phase at ~370 °C. The Al/CuO NPs without PW were remained at > 370 °C, resulting in the aluminothermic reaction between Al and CuO at 450–600 °C. The total heat energy, which was determined by integrating the positive exothermic heat flow curves, was significantly decreased with increasing the PW contents for both air and Ar atmospheres as shown in Fig. 6c. The higher heat flows observed in the air than Ar atmosphere were originated from the oxygen-rich and PW oxidation conditions. This suggests that the addition of a controlled amount of PW (≤ 20 vol%) to the Al/CuO composite pellet was required to minimize the loss of overall exothermic reaction energy of the Al/CuO composite matrix. The presence of excessive PW in the Al/CuO composite can significantly deteriorate this reaction by increasing the coating thickness and interfering with aluminothermic reactions.

Figure 7a shows pressure traces of the PW/Al/CuO composite pellets ignited in the closed PCT system used to examine the effect of PW content on the explosion pressure of the pellets. The maximum pressure generated by the explosion of the composite pellets increased with increasing PW content due to rapid vaporization of the binder. Figure 7b shows the pressurization rates of various PW/Al/CuO pellets, which was determined by calculating the ratio of the maximum pressure to the rise time. Steeper slopes in the time–pressure graphs indicate larger pressurization rates. For PW contents ≤ 20 vol%, the pressurization rates of the composite pellets were higher than that of Al/CuO composite pellet as the critical PW content promoted pellet combustion to some extent. However, the pressurization rate significantly decreased with increasing PW content > 30 vol%, deteriorating the combustion properties of the pellets due to the binder interfering with the thermochemical reaction.

To examine the relative water permeability of the pellets, we performed contact angle measurements for all PW/Al/CuO composite pellets, as shown in Fig. 8. It was clearly observed that the average contact angle of the surface of the pellet significantly increased with increasing PW content up to ~20 vol%, and then gradually plateaued with PW contents of 30–50 vol% in the Al/CuO matrix. This suggests that porosity in the Al/CuO matrix was filled with PW binder, increasing the hydrophobicity of the coating and protecting the PW-coated Al/CuO composite pellets from severe oxidation by water molecules present in the reaction atmosphere.

To examine the effect of relative humidity (RH) on the combustion properties of PW/Al/CuO pellets, the different composite pellets were exposed to a fixed RH of 50% for 10 min, 1 d, 10 d, 20 d, and 30 d. Then, the evolution of their combustion properties was analyzed (Fig. 9a). The burn rate of the composite pellets generally decreased with increasing PW content ($\geq$ 10 vol%) after exposure to 50% RH for periods of 10 min to 30 d. However, it is interesting to note that Al/CuO composite pellets without the addition of binder could not be successfully ignited after the Al/CuO pellets were exposed to RH 50% for longer than 1 d. This suggests that the Al NPs were significantly humidified and oxidized by water molecules infiltrating the pores between the Al/CuO matrix, eventually resulting in ignition failure. Therefore, the presence of PW was shown to protect the Al/CuO matrix from severe wetting and oxidation. In addition, the total burning time of PW/Al/CuO composite pellets generally increased with increasing PW content, regardless of the duration of moisture exposure (Fig. 9b). This suggests that the PW binder played a key role as both a hydrophobic and energetic agent; hence, it was able to reliably maintain or even enhance various combustion properties of Al/CuO composite pellets when added in optimized quantities.

4. Conclusions

We examined the effect of PW binder content on the combustion properties and surface protection of Al/CuO NP-based composite pellets. The presence of PW separated the Al and CuO NPs to some extent, resulting in degradation of the aluminothermic reaction and a reduced burn rate of the pellets with increasing PW content. However, a critical amount of PW < 20 vol% showed various advantages, including, facile compaction of the Al/CuO composite pellets, and enhanced total heat energy, maximum pressure, and pressurization rate generated by the ignition of PW/Al/CuO composite pellets. This suggests that PW affected both the lubrication and energetic properties. In addition, the presence of PW was shown to effectively protect Al/CuO composite pellets from severe wetting and oxidation during exposure to humidity, suggesting that PW is also an effective hydrophobic agent. Thus, the long-term storage and handling stability of Al/CuO composite pellets under high relative humidity conditions can be significantly improved by the addition of PW.

Declarations of interest

None.

Acknowledgments

This research was supported by the Civil & Military Technology Cooperation Program through the National Research Foundation of Korea (NRF), funded by the Ministry of Science and ICT (No. 2013M3C1A9055407). This research was also partially supported by the Basic Science Research Program through the National Research Foundation of Korea, (NRF) funded by the Ministry of Education (No. 2016R1A6A3A11935550).

Supplementary materials

Supplementary material associated with this article can be found, in the online version, at doi:10.1016/j.combustflame.2018.09.010.

References

[1] K.J. Blobaum, M.E. Reiss, J.M. Plitzko, T.P. Weihs, Deposition and characterization of a self-propagating CuO_X/Al thermite reaction in a multilayer foil geometry, J. Appl. Phys. 94 (5) (2003) 2915–2922.
[2] J.L. Cheng, H.H. Hng, H.Y. Ng, P.C. Soon, Y.W. Lee, Synthesis and characterization of self-assembled nanoenergetic Al-Fe_2O_3 thermite system, J. Phys. Chem. Solids 71 (2) (2010) 90–94.
[3] S.F. Son, B.W. Asay, T.J. Foley, R.A. Yetter, M.H. Wu, G.A. Risha, Combustion of nanoscale Al/MoO_3 thermite in microchannels, J. Propul. Power 23 (4) (2007) 715–721.
[4] J.Y. Ahn, W.D. Kim, K. Cho, K, D. Lee, S.H. Kim, Effect of metal oxide nanostructures on the explosive property of metastable intermolecular composite particles, Powder Technol. 211 (1) (2011) 65–71.
[5] S.H. Kim, M.R. Zachariah, Enhancing the rate of energy release from nanoenergetic materials by electrostatically enhanced assembly, Adv. Mater. 16 (20) (2004) 1821–1825.
[6] J.Y. Malchi, T.J. Foley, R.A. Yetter, Electrostatically self-assembled nanocomposite reactive microspheres, ACS Appl. Mater. Inter. 1 (11) (2009) 2420–2423.
[7] P.F. Pagoria, G.S. Lee, A.R. Mitchell, R.D. Schmidt, A review of energetic materials synthesis, Thermochim. Acta 384 (1–2) (2002) 187–204.
[8] X. Zhou, M. Torabi, J. Lu, R. Shen, K. Zhang, Nanostructured energetic composites: Synthesis, ignition/combustion modeling, and applications, ACS Appl. Mater. Inter. 6 (5) (2014) 3058–3074.
[9] K.J. Kim, H. Jung, J.H. Kim, N.S. Jang, J.M. Kim, S.H. Kim, Nanoenergetic material-on-multiwalled carbon nanotubes paper chip as compact and flexible igniter, Carbon 114 (2017) 217–223.
[10] J.H. Kim, J.Y. Ahn, H.S. Park, S.H. Kim, Optical ignition of nanoenergetic materials: The role of single-walled carbon nanotubes as potential optical igniters, Combust. Flame 160 (4) (2013) 830–834.
[11] J.Y. Ahn, J.H. Kim, J.M. Kim, S.H. Kim, Effect of oxidizer nanostructures on propulsion forces generated by thermal ignition of nano-aluminum-based propellants, J. Nanosci. Nanotech. 13 (10) (2013) 7037–7041.
[12] J.H. Kim, M.H. Cho, K.J. Kim, S.H. Kim, Laser ignition and controlled explosion of nanoenergetic materials: The role of multi-walled carbon nanotubes, Carbon 118 (2017) 268–277.
[13] J. Shen, Z. Qiao, K. Zhang, J. Wang, F. Nie, Effects of nano-Ag on the combustion process of Al–CuO metastable intermolecular composite, Appl. Therm. Eng. 62 (2) (2014) 732–737.
[14] A. Ambekar, J.J. Yoh, A reduced order model for prediction of the burning rates of multicomponent pyrotechnic propellants, Appl. Therm. Eng. 130 (2018) 492–500.
[15] A. Prakash, A.V. McCormick, M.R. Zachariah, Aero-Sol− Gel synthesis of nanoporous iron-oxide particles: A potential oxidizer for nanoenergetic materials, Chem. Mater. 16 (8) (2004) 1466–1471.
[16] B. Mehendale, R. Shende, S. Subramanian, S. Gangopadhyay, P. Redner, D. Kapoor, S. Nicolich, Nanoenergetic composite of mesoporous iron oxide and aluminum nanoparticles, J. Energ. Mater. 24 (4) (2006) 341–360.
[17] A. Prakash, A.V. McCormick, M.R. Zachariah, Tuning the reactivity of energetic nanoparticles by creation of a core−shell nanostructure, Nano Lett. 5 (7) (2005) 1357–1360.
[18] S.M. Umbrajkar, M. Schoenitz, E.L. Dreizin, Exothermic reactions in Al–CuO nanocomposites, Thermochim. Acta 451 (1–2) (2006) 34–43.
[19] S. Valliappan, J. Swiatkiewicz, J.A. Puszynski, Reactivity of aluminum nanopowders with metal oxides, Powder Technol. 156 (2–3) (2005) 164–169.
[20] J.L. Cheng, H.H. Hng, H.Y. Ng, P.C. Soon, Y.W. Lee, Synthesis and characterization of self-assembled nanoenergetic Al–Fe_2O_3 thermite system, J. Phys Chem. Solids 71 (2) (2010) 90–94.
[21] M.L. Pantoya, J.J. Granier, Combustion behavior of highly energetic thermites: Nano versus micron composites, Propell. Explos. Pyrot. 30 (1) (2005) 53–62.
[22] K. Park, D. Lee, A. Rai, D. Mukherjee, M.R. Zachariah, Size resolved kinetic measurements of aluminum nanoparticle oxidation with single particle mass spectrometry, J. Phys. Chem. B 109 (15) (2005) 7290–7299.
[23] R. Shende, S. Subramanian, S. Hasan, S. Apperson, R. Thiruvengadathan, K. Gangopadhyay, S. Gangopadhyay, P. Redner, D. Kapoor, S. Nicolich, W. Balas, Nanoenergetic composites of CuO nanorods, nanowires, and Al-nanoparticles, Propell. Explos. Pyrot. 33 (2) (2008) 122–130.
[24] J.Y. Ahn, J.H. Kim, J.M. Kim, D.W. Lee, J.K. Park, D.G Lee, S.H. Kim, Combustion characteristics of high-energy Al/CuO composite powders: The role of oxidizer structure and pellet density, Powder Technol 241 (2013) 67–73.
[25] Y. Xia, P. Yang, Chemistry and physics of nanowires, Adv. Mater. 15 (5) (2003) 351–352.
[26] E.C. Walter, B.J. Murray, F. Favier, R.M. Penner, "Beaded" bimetallic nanowires: Wiring nanoparticles of metal 1 using nanowires of metal 2, Adv. Mater. 15 (5) (2003) 396–399.
[27] Z.L. Wang, Nanobelts, nanowires, and nanodiskettes of semiconducting oxides—from materials to nanodevices, Adv. Mater. 15 (5) (2003) 432–436.

[28] Y. Xia, P. Yang, Y. Sun, Y. Wu, B. Mayers, B. Gates, Y. Yin, F. Kim, H. Yan, One-dimensional nanostructures: Synthesis, characterization, and applications, Adv. Mater. 15 (5) (2003) 353–389.
[29] C. Rossi, K. Zhang, D. Esteve, P. Alphonse, Nanoenergetic Materials for MEMS: A review, J. Microelectromech. S. 16 (4) (2007) 919–931.
[30] C. Badila, M. Schoenitz, X. Zhu, E.L. Dreizin, Nanocomposite thermite powders prepared by cryomilling, J. Alloy. Compd. 488 (1) (2009) 386–391.
[31] T.R. Sippel, S.F. Son, L.J. Groven, Aluminum agglomeration reduction in a composite propellant using tailored Al/PTFE particles, Combust. Flame 161 (1) (2014) 311–321.
[32] R.J. Jouet, A.D. Warren, D.M. Rosenberg, V.J. Bellitto, K. Park, M.R. Zachariah, Surface passivation of bare aluminum nanoparticles using perfluoroalkyl carboxylic acid, Chem. Mater. 17 (2005) 2987–2996.
[33] S.W. Chung, E.A. Guliants, C.E. Bunker, D.W. Hammerstroem, Y. Deng, M.A. Burgers, P.A. Jelliss, S.W. Buckner, Capping and passivation of aluminum nanoparticles using alkyl-substituted epoxides, Langmuir 25 (2009) 8883–8887.
[34] M.A. Trunov, M. Schoenitz, X. Zhu, E.L. Dreizin, Effect of polymorphic phase transformations in Al_2O_3 film on oxidation kinetics of aluminum powders, Combust. Flame 140 (2005) 310–318.
[35] S. Hasani, M. Panjepour, M. Shamanian, The oxidation mechanism of pure aluminum powder particles, Oxid. Met. 78 (2012) 179–195.
[36] P.A. Jelliss, S.W. Buckner, B.J. Thomas, US Patent Application No. 14/259859. Washington, DC: US Patent and Trademark Office (2015).
[37] S. Gangopadhyay, R. Shende, S. Subramanian, K. Gangopadhyay, S. Hasan, US Patent No. 7927437. Washington, DC: US Patent and Trademark Office (2011).